IEEE Access
Multidisciplinary | Rapid Review | Open Access Journal

Received August 30, 2021, accepted October 7, 2021, date of publication October 19, 2021, date of current version October 27, 2021.

Digital Object Identifier 10.1109/ACCESS.2021.3121548

Ancillary Voltage Control Design for Adaptive Tracking Performance of Microgrid Coupled With Industrial Loads

SUBRATA K. SARKER[1], SHAHRIAR RAHMAN FAHIM[2], (Member, IEEE), NILOY SARKER[2], (Member, IEEE), KAZI ZAKARIA TAYEF[2], ABU BAKAR SIDDIQUE[3], DRISTI DATTA[4], M. A. PARVEZ MAHMUD[5], (Member, IEEE), MD. FATIN ISHRAQUE[6], SAJAL K. DAS[1], MD RABIUL ISLAM SARKER[7], SK. A. SHEZAN[8], AND ZIAUR RAHMAN[9], (Graduate Student Member, IEEE)

[1]Department of Mechatronic Engineering, Rajshahi University of Engineering and Technology, Rajshahi 6204, Bangladesh
[2]Department of Electrical and Electronic Engineering, American International University-Bangladesh, Dhaka 1229, Bangladesh
[3]Faculty of Energy Systems and Nuclear Science, Ontario Tech University, Oshawa, ON L1G 0C5, Canada
[4]Department of Electrical and Electronic Engineering, Uttara University, Dhaka 1230, Bangladesh
[5]School of Engineering, Deakin University, Geelong, VIC 3216, Australia
[6]Department of Electrical, Electronic and Communication Engineering, Pabna University of Science and Technology, Pabna 6600, Bangladesh
[7]Department of Mechanical Engineering, Rajshahi University of Engineering and Technology, Rajshahi 6204, Bangladesh
[8]Department of Electrical Engineering, Engineering Institute of Technology, Melbourne Campus, Melbourne, VIC 3001, Australia
[9]Department of Information and Communication Technology, Mawlana Bhashani Science and Technology University, Tangail 1902, Bangladesh

Corresponding author: Subrata K. Sarker (subrata@mte.ruet.ac.bd)

This work was supported by the School of Engineering, Deakin University.

ABSTRACT Although the utilizing of renewable energy sources (RESs) in microgrid (MG) offers a recognized solution to meet the increasing demand, it's performance depend on various meteorological factors of RESs. Again, the functioning of MGs is often affected with certain industrial load dynamics which allowing them to alter the operating region and tracking function of the MGs. The above-mentioned challenges motivate us to design the ancillary voltage control design for enabling the MGs to provide adaptive transient and tracking voltage responses over the changes of various factors like weather, consumer demand, and industrial loads. Firstly, we design an intelligent adaptive control (IAC) framework made by merging with proportional-integral (PI) regulator and artificial neural network (ANN) to sustain the regulated common bus voltage over the mentioned changes. The regulated bus voltage is forwarded to operate the industrial loads via the regulation of inverter-based secondary network (SN). A study on the variation of weather condition and consumer demand is done to show the efficacy of the IAC framework. Secondly, we propose a novel fixed control structure named model reference modified fractional-order PID (MR-F0PID) regulator to maintain the high tracking response of the MG via the control of inverter associated with the SNs. The tracking competency of this fixed control framework is analyzed over the running of a few industrial loads dynamics associated with single-phase inverter based SN and results are compared with the other related existing controllers. Moreover, a mathematical analysis for mapping the stable region is completed here to track down the closed-loop stability area. As a further study, the three-phase inverter based SN associated with several three-phase industrial load is also considered with the same DC bus and analyzed to observe the competency of the proposed fixed MR-FOPID control framework.

INDEX TERMS Adaptive controller, DC bus voltage stabilizer, fractional-order regulator, microgrid control and PV source.

I. INTRODUCTION

In the modern era of automation, energy utilization is expanding step by step. The increasing energy consumption produces diverse compulsion on the traditional power system and enables the engineering community to discover an elective way for energy production [1]. Since our natural resources are limited, the alternative way demands the penetration of sustainable energy sources with the traditional power system [2]. Microgrid (MG) enables a way of

The associate editor coordinating the review of this manuscript and approving it for publication was Amedeo Andreotti.

producing electricity using RERs like water, sun-oriented, air, and different types of renewable energy. It can offer the remarkable development of load interest inside limited foundation cost and give a dependable, secure, and sustainable environmentally friendly power energy [3]–[6]. A general form of microgrid contains the sustainable energy sources, point of common coupling (PCC), power electronics inverter/converte, loads and so on. It can drive the load in two modes: off-grid and grid-connected mode [7], [8].

During the grid-connected mode, the operation of MG is largely dependent on the main AC grid that may increase the transmission and investment loss when the power supplies in a place located far from the generation end [9]. Accordingly, the islanded mode of MG operation relies on its prime mover performance that are often named as distributed generations (DGs) unit [10]. The expanding utilization of DGs unit conducts undesirable responses of the MG framework in off-grid condition as they are normally stochastic. Proper functioning of these DGs unit demands the fixed speed of the wind, strength of solar, and many more [11], [12].

Any distortion of these meteorological factors may create noise in the form of disturbances and packet losses that initiates an imbalance performance of the MG system [13], [14]. Several linear and nonlinear control strategies are already studied to regulate the stable performance of the MG.

A linear Droop regulation method is developed in [15], where a resistance is considered virtually at the load terminal of the MG. The lack of proper tuning of the droop coefficients can produce more oscillatory performance against the variation of operating conditions. The study of nonlinear sliding mode control (SMC) strategy can deal with the above issue and show stable performance [2], [16]. Although the SMC deals with the stable performance under various operating regions, it neglects the impact of generation changes. Thus, the design of an adaptive controller is still of interest to the researcher. The regulation of the stable performance over the change of weather factors cannot guarantee the tracking performance for the industrial loads. The operation of these loads demands the inclusion of the inverter-based secondary network (ISN)/distribution system in the MG premises [17]. However, the addition of inverter based SNs may produce nonlinear element due to nature of inverter that leads the loads alongside uncertainties. Furthermore, the un-modeled load elements in MG area produces external noises that may hamper the tracking performance [18]. Consequently, the regulation of MG tracking response has prompted an arising research region and implementation of a reliable control scheme is required to confirm the adaptive tracking performance over the industrial loads.

Extensive studies are already done to design an appropriate control framework for ensuring the improved tracking competency of the MG under the change of loads. Among them, proportional-integral-derivative (PID) is getting much popularity due to its simplicity [19], [20]. In [10], [20], authors use various methods like Chien-Hrones-Reswick (CHR), Ziegler-Nichols, Cohen-Coon and linear-matrix-inequality (LMI) to develop the PID controller for the improvement of MG tracking performance. Here, the controller is designed for only the single-phase industrial loads. However, the response of the above designed PID controller using these methods may suffer low tracking over the operation of multi-variable loads as the PID controller is highly sensitive to parameter changes.

Linear quadratic regulator (LQR) is used in MG to execute swift and improved performance [21]–[23]. The regulator accomplishes swift response under the region of the RLC network associated with the MG area parallelly. Plant model changes and estimator inclusion complexity reduces the effectiveness and restricts its application here. In [24]–[26], consider the model predictive controller (MPC) for the stabilization of MG voltage and its current. It uses a multivariable controlling approach with a dynamic plant model and optimized receding estimation horizon. The main characteristic of MPC is that it does not need the current time slots to be optimized for future time slots explanation. Lower flexibility's and mathematical model translation complexities reduce the usage of MPC approach.

A blended regulator, which consolidates a PI regulator and a resonant regulator (RR), has been contemplate to acquire zero steady-state error by controlling the grid harmonics [5], [27]. It proceeds as a low pass regulator in the region of high frequency and makes a lower control margin. This lower control margin abbreviates the utilization of this regulator. Another control algorithm named adaptive sliding mode control (ASMC) has been studied to mitigate the harmonics produced due to plant current [28]. It predicts the active and re-active powers and ensures the maximum utilization of Balloon-borne Experiment with Superconducting Spectrometer (BESS) capacity. By moving the load between the generating frameworks, the ASMC can maintain the power balance. It never permits the expansion of DC-interface voltage over the greatest float rate voltage by eliminating all possible overshoot and undershoot problems [29]. But, the response competency of ASMC may be suffered when a group of loads are placed into the system. Decentralized [30]–[32] and distributed [33] regulator are utilized to procure the controlled sharing current and voltage appropriately. Diverse parameter states are observed by a distant sensing element and the data is forwarded to the regulator unit via a low transfer speed framework. Slow reaction because of this low data transfer capacity lessens these regulators' application. An expert control structure named Fuzzy regulator is developed by contemplating a list of true or false logic condition [34], [35]. A process to acquire the fuzzy value from the regulator crisp input by using the considered membership functions is called fuzzification. It is viable towards the adjustment of plant elements, however the use of this regulator relies upon the planner/expert information. The absence of appropriate information might cause to conduct a lower performance.

The limitations exposed in previous literature motivate us to develop the required control models for balanced and adaptive tracking response of the MG over the unknown

input and output parameters. These obscure parameters are the consequences of abrupt variations of consumer demand, sustainable energy parameters like irradiance and temperature for solar-oriented generating system, and loads power that results in offer the inferior performance. This paper deals with the design of the ancillary voltage control models for adaptive tracking performance of the MG under the study of the above unknown parameters. A preliminary version of this work is presented in [36] where the proposed control framework deals with the tracking problems related to the load variations. This is done by controlling the multi-variable SN associated with multi-variable industrial loads. However, this study neglects the variation of PV parameters, i.e., temperature and irradiance, and consumer demand. The change of these factors produces a variety of performances in the MG load premises as they serve a source of input power for the load connected SNs. This research gap inspires us to extend the work by incorporating intelligent adaptive control (IAC) framework with the control framework used in [36]. The reason behind the use of IAC is to offer a stable source of input power for SNs over the changes of PV parameters and consumer demand. Additionally, the extended version considers a couple of SNs to determine the efficacy of the MR-FOPID controller. The main technical contribution of this paper is divided as three-folded.

- Firstly, we develop a novel intelligent adaptive control (IAC) approach based on the artificial neural network (ANN) and the conventional PI controller to confirm the stable DC bus voltage within a certain range, typically 300-2000 V, over the change in meteorological factors of PV. The function of ANN is to estimate the voltage of the common bus in accordance with the desired common bus voltage, temperature and irradiance, and make error voltage between the consumer demand and actual bus voltage. At the same time, the PI controller stabilizes/controls the error by enabling the DC-DC bi-directional converter which allows exchanging power between PV and the main AC grid, and offers a source of constant input voltage to drive the SNs.
- Secondly, we propose a novel fixed control structure known as MR-F0PID controller to regulate the inverters associated with SNs, allowing them to provide adaptive reliable tracking performance under the study of various industrial loads.
- Thirdly, a theoretical stability conditions for the proposed MR-FOPID control framework is also established to explore the closed-loop stability margin.

The inverter control method appeared with the secondary networks contains a reference model, nominal plant, adaptive mechanism, and the control unit. A fractional order PID control unit is merged with the adaptive mechanism to reduce the tracking error produced from the expected and actual load voltage, and ensure the flawless tracking operation for the various load dynamics.

The arrangement of the rest of the paper is split into four sections. A short investigation about the modelling of secondary network, designing of intelligent adaptive stabilizer and modelling of renewable energy source is reported in Section 2. In section 3, the mathematical model of proposed MR-FOPID framework with required stability analysis for SN control is discussed. The assessment of the designed controller over the single and three phase SN is investigated in Section 4. The concluding remarks of this paper are shown in Section 5.

TABLE 1. Qualitative comparison between the ANN, IC and P&O based MPPT [37], [38].

Reason	P&O	IC	ANN
Convergence Speed	Average	Low	High
Support Scalability	No	No	Yes
Oscillation around MPP	Yes	Yes	No
Drifting problem	Yes	No	No
Reliability under partial shedding	Low	Medium	High
Algorithm complexity	Medium	Medium	Low

II. SYSTEM INVESTIGATION

A. STUDIED MICROGRID SYSTEM

The reason behind the studied of this type of MG is to confirm the improved operation of the renewable energy resources against the number of loads dynamic. A circuit depicted in Fig. 1 describes the model of the considered MG where a common DC terminology performs as the bridge to connect a sustainable energy source (SES) like PV, a single-phase secondary network and primary AC network. The operation of the AC network along with the DC bus demands a three phase bi-directional converter that empowers the MG framework to interchange power in the middle of the AC and DC side. In this study, the primary AC network plays a role to stabilize the bus voltage through the taking and providing power when the generated power from the SES is greater or smaller than the reference voltage of the DC bus. A couple of SNs is straightforwardly fixed with the relating DC bus by using the filter and power electronics equipment's like voltage source inverters (VSIs). The output voltage from the VSIs is utilized to lead the loads associated with the SNs. The selected input for the main and SNs are 3 KV and 300 V, respectively.

An MG framework provides power in grid-off and grid-on modes. In the state of grid-on, a three-phase bi-directional converter is needed to serve the stable common bus voltage, while a source of renewable energy acts as a prime mover to drive the MG in islanded mode. In this study, the PV array module is used as sustainable energy source connected with common bus through a boost converter which aims to take out the maximum power (MP) from the solar-oriented system. Here, an ANN is placed here to enable the converter for tracking the MP point. The reasons behind the use of ANN over the others methods are listed in Table 1. At the point when the power of the solar-oriented system is more prominent than the overall power ingested at the common bus terminal, the two-way converter infuses power from the DC

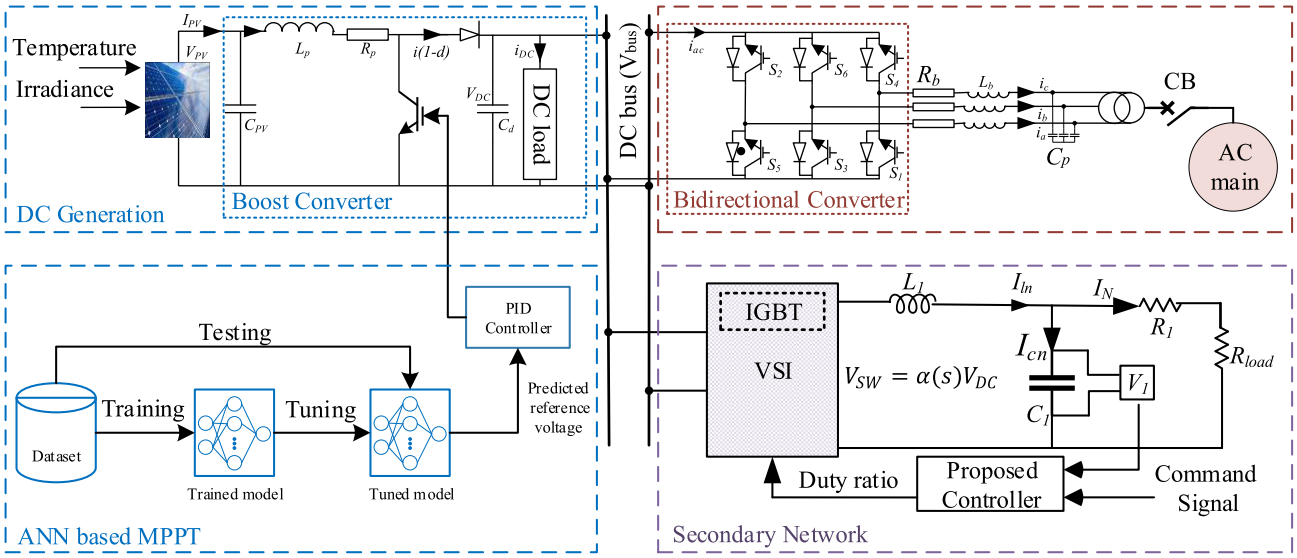

FIGURE 1. Circuit diagram of microgrid system consisting of inverter-based secondary network.

TABLE 2. PV module specification.

Parameter	Description
N_s	Number of series cells
I_{photon}	Generated Current by Incident Photon
I_{scc}	Cell short circuit current
K_i	Temp. coefficient for SHort circuit current
T	Working temperature of the cell
T_r	Reference temperature
λ	Solar irradiaiton (kW/sq. m)
I_{rsc}	Reversely Saturated Current of cell
q	Electron Charge
V_{diode}	Voltage across the diode
n	Model parameter (1.5 for Si Cell)
K	Boltzmann Constant
I_{csrr}	Cell Saturated Current at Temp T_r
E_g	Band gap energy for the used semiconductor
V_{pv}	Output voltage of the cell

side to the AC framework while going about as an inverter. Then again, if the level of all out power at the same common terminal is smaller than the essential power, the converter infuses power from the fundamental AC framework to the DC part.

On account of the SN activity, an enormous amount of harmonics might create during the changing of DC to AC voltage. A load having with inductive nature is utilized to keep up with the stability of exchanging methods of voltage. The utilization of this lagging load might request a large amount current from the common bus. Accordingly, an extra capacitor is utilized to cover the requested current without enabling the requirement for an additional converter in input side. The mix of a capacitor and inductor forms a filter to navigate the SN that keeps the consistent DC interface voltage as well as builds the infused power in the SNs load terminal.

1) MODELING OF PV SOURCE

An electrical equivalent circuit model for PV panel with load is exposed in Fig. 2 consisting of a solar source and a

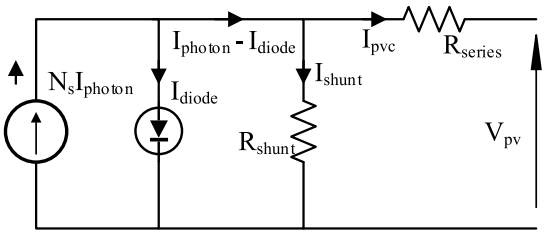

FIGURE 2. An electrical equivalent circuit model for PV panel with load.

diode operated series resistance R_{series}. A shunt diode resistance R_{shunt} is associated in corresponding with a diode that empowers a detour approach to create the current. The output current I_{pvc} from PV cell is represented as,

$$I_{pvc} = N_s I_{photon} - I_{diode} - I_{shunt}, \tag{1}$$

Here, the generated current by incident photon

$$I_{photon} = [I_{scc} + K_i(T - T_r)]\lambda, \tag{2}$$

where,

$$\lambda = \frac{G}{1000},$$

Here, G represents the global irradiance falling perpendicular on the surface. Now, the term I_{diode}, I_{rsc} and I_{shunt} defines the diode current, reverse saturation current of PV cell and current across the shunt resistance can be written as

$$I_{diode} = I_{rsc}[exp(\frac{q(V_{diode} + IR_{series})}{nKT}) - 1], \tag{3}$$

$$I_{rsc} = I_{csrr}(\frac{T}{T_r})^3[exp[\frac{qE_g(\frac{1}{T_r} - \frac{1}{T})}{nK}], \tag{4}$$

and

$$I_{shunt} = \frac{V_{pv} + I_{pvc}R_{series}}{R_{shunt}}. \tag{5}$$

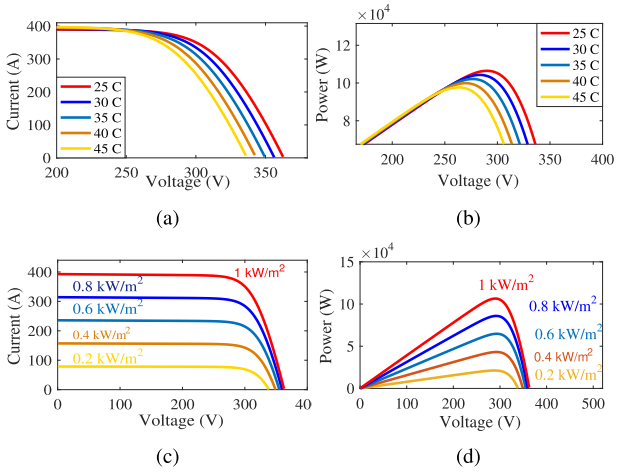

FIGURE 3. (a) I-V, and (b) P-V characteristics curve for different temperature level and (c) I-V, and (d) P-V characteristics curve for different irradiance.

Now putting the values of (2) and (3) into (1) we get,

$$I_{pvc} = N_s I_{photon} - N_p I_{rsc}[exp(\frac{q(V_{diode} + IR_{series})}{nKT}) - 1] - \frac{V_{pv} + I_{pvc}R_{series}}{R_{shunt}}.$$

The notations of the designed parameters for the PV system are presented in Table 2. The value of these parameters are taken from [1] that are chosen utilizing the models of the genuine PV framework so that the considered solar-oriented framework meets the every condition to run in the practical environment. The I-V and P-V curve for the studied PV panel made with parameters value exposed in [1] is illustrated in Fig. 3 under the experiment of various temperatures and irradiance.

B. DESIGN INTELLIGENT ADAPTIVE CONTROL FRAMEWORK FOR BUS VOLTAGE STABILIZER

A stable source of voltage with the variation of consumer demand and PV parameters, i.e.,temperature and irradiance, is the primary condition to ensure the reliable operation of SN. Here, the adaptive stable common bus voltage is prolonged through the design of an intelligent adaptive control (IAC) framework as shown in Fig. 4, which carries the combination of an ANN and PI regulator. The function of ANN is to estimate the output DC bus voltage based on temperature, irradiance and reference common bus terminal voltage. At the same time, the PI reduces the error produced from the comparison of estimated and consumer demand DC bus voltage, and allows tracking performance through the controlling of bi-directional converter which permits exchanging the power between PV and primary AC grid when excess or needy power is produced. The details process are discussed in the following section.

1) ARTIFICIAL NEURAL NETWORK

The artificial neural networks (ANNs) are motivated by the complex neural system that forms an animal brain [39], [40]. Like the biological interaction between billions and trillions of neurons in an animal brain, the ANNs process the information. The information which is taken as an input is transmitted through nodes in different layers to the output. The nodes or the neurons process the inputs linearly. Thus, the non-linearity is added to the output of the ANN by using the activation function. In the proposed system, the ReLU activation function [41] is utilized and the inputs to the ANN are processed as:

$$O_{neuron} = \sum_{i=1}^{i=n} W_i \times x_i + \alpha \tag{6}$$

Here, x indicates the inputs and W signifies the weights. α represents the learning rate. The back-propagation algorithm along with the adam optimizer [42] is placed here to train the three-layer ANN architecture. The information for training the ANN architecture are generated by varying the levels of PV parameters, V_{DC}^{ref} and i_d^{ref}. The total generated data are split into two sets: testing and training group with a value of 7:3. Once the neural network is trained with a sufficient amount of data, it can predict the output and can set coordination between the solar module and the AC main grid. The predicted voltage for the changes of solar input parameters is shown in Fig. 5. Here, the minimum (300V) and maximum limit (2000V) of preparing data are just used as the consumer demand voltage to test the adaptive capability of the IAC in case of voltage tracking performance and its outcomes are exposed in Fig. 6. The regulated outcomes confirm that the IAC is competent of delivering the adaptive tracking response according to the demanded voltage. The regulated tracking voltage from the DC bus terminal is used as the source of input voltage for the SNs. Although there is a ripple content in Fig. 6 and it is occurred when the system first received the input (temperature and irradiance) at 0.0s, a voltage transient occurs and the controller, i.e., the ANN combined with PI begins to regulate the voltage and takes approximately 0.27s to settle down to steady-state after finishing the learning process. However, such variation of DC bus voltage in transient period is independent with the SN voltage regulation due to the development MR-FOPID controller.

C. MATHEMATICAL MODELING OF SNs

Consider I_{ln} is the inductor current signal going across the SN that can be written as,

$$V_l(t) = L_1 \frac{dI_{ln}(t)}{dt},$$

Applying Laplace transform, we get

$$I_{ln}(s) = \frac{V_L(s)}{sL_1} = \frac{V_{sw}(s) - V_1(s)}{sL_1}. \tag{7}$$

In (7), the switching voltage $V_{sw}(s)$ is carrying the multiplication of the $\alpha(s)$ duty cycle and voltage from the common bus terminal $V_{bus}(s)$.

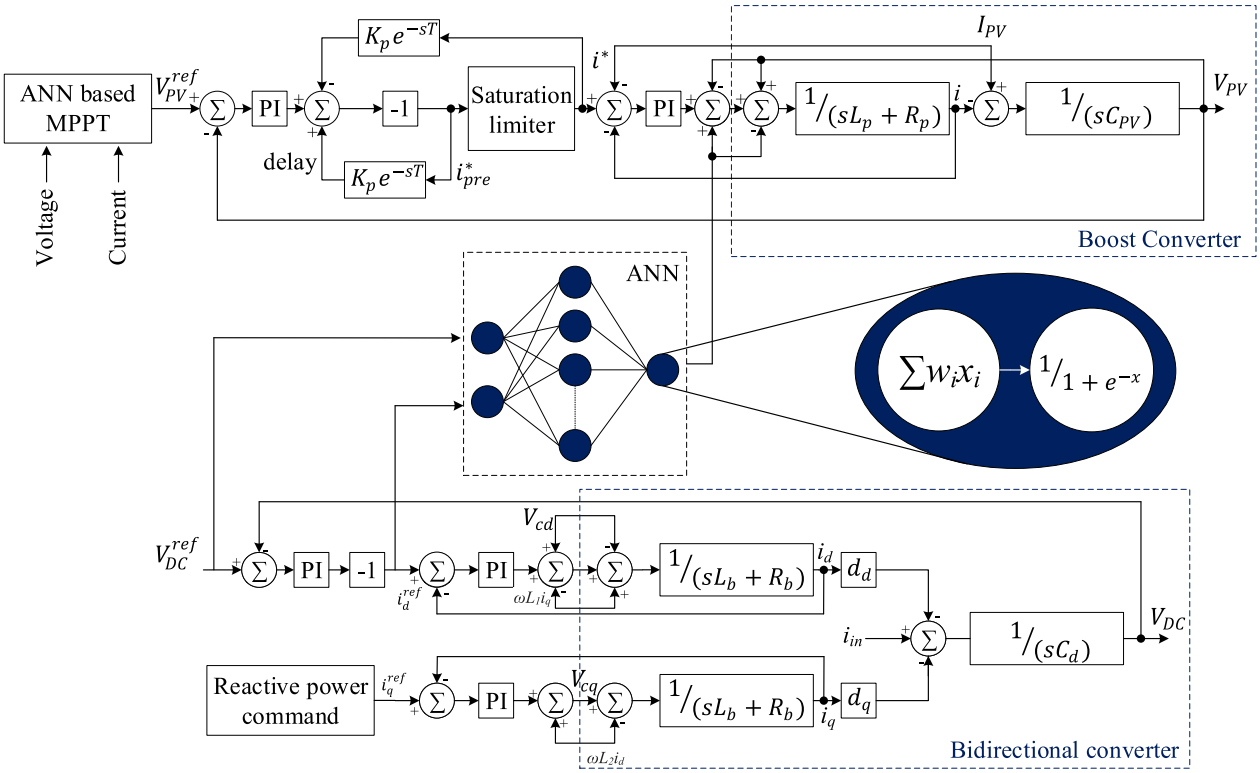

FIGURE 4. A schematic diagram of proposed intelligent adaptive bus voltage stabilizer.

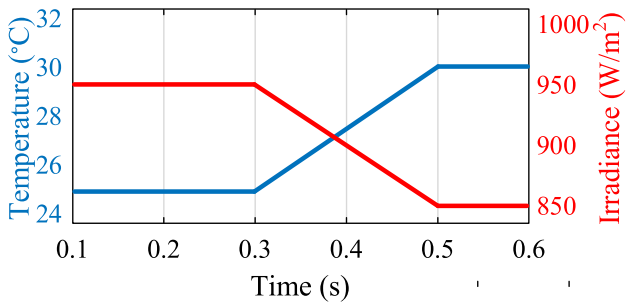

FIGURE 5. Input temperature and irradiance for PV panel.

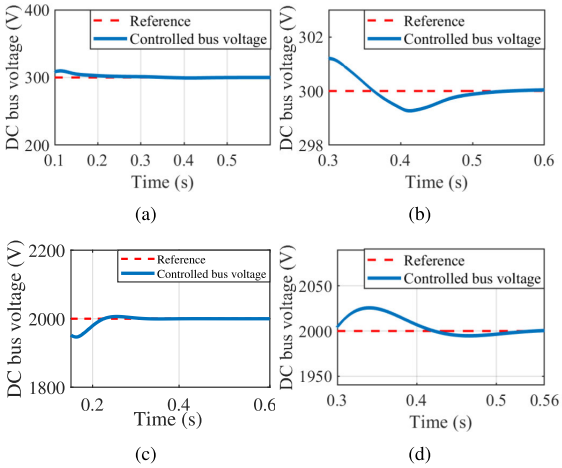

FIGURE 6. Regulation of DC bus voltage using IAC for (a) minimum value of generated dataset, (b) zoom version of (a), (c) maximum value of generated dataset and (d) zoom version of (c).

Accordingly, the capacitor voltage V_1, which is mainly the distribution voltage among the load that needs to be considered as the controlled parameter, passing through the SN voltage can be obtained as following,

$$\frac{dV_1}{dt} = \frac{1}{C_1(t)} I_{cn}(t),$$

Applying Laplace transform, we get

$$V_1(s) = \frac{1}{sC_1(s)} I_{cn}(s) = \frac{1}{sC_1(s)} (I_{ln}(s) - I_N(s)) \qquad (8)$$

In (8), I_{cn} and I_N describes the capacitor current and load current, respectively. Now, we can explore the control model for SN system by using (7) and (8):

$$\frac{d}{dt}\begin{bmatrix} I_{ln} \\ V_1 \end{bmatrix} = \begin{bmatrix} 0 & -\frac{1}{L_1} \\ \frac{1}{C_1} & 0 \end{bmatrix} \begin{bmatrix} I_{ln} \\ V_1 \end{bmatrix} + \begin{bmatrix} \frac{1}{L_1} \\ 0 \end{bmatrix} [V_{sw}] + \begin{bmatrix} 0 \\ -\frac{1}{C_1} \end{bmatrix} [I_N],$$

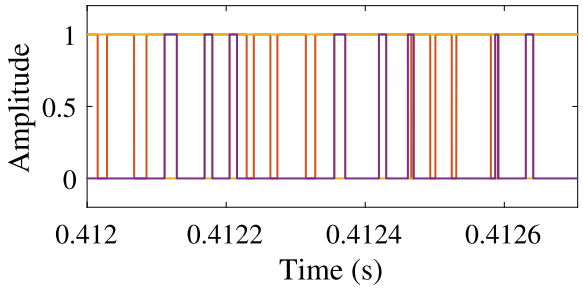

FIGURE 7. Switching pulses for voltage sources inverter (VSI) associated with secondary networks.

and the SN output is:

$$y = \begin{bmatrix} V_1 \end{bmatrix} = \begin{bmatrix} 0 & 1 \end{bmatrix} \begin{bmatrix} I_{ln} \\ V_1 \end{bmatrix}.$$

which can be considered as $T(s) = T_G(s) + \triangle(s)$, where the transfer function of the nominal system $T_G(s) = C(sI - A)^{-1}B + D$. Here, $A = \begin{bmatrix} 0 & -\frac{1}{L_1} \\ \frac{1}{C_1} & 0 \end{bmatrix}$ is the single-phase SN matrix, $B = \begin{bmatrix} \frac{1}{C_1} \\ 0 \end{bmatrix}$ exposes the contribution matrix, $C = \begin{bmatrix} 0 & 1 \end{bmatrix}$ indicates the SN output matrix, and the transition matrix $D = 0$. The term $\triangle(s) = \begin{bmatrix} 0 \\ -\frac{1}{C_1} \end{bmatrix} I_N(s)$ indicates the uncertainty added with the system output from the input. The parameters for SN are chosen to remember that it can behave like a practical MG which can consume power from common bus and infuse it to the load terminal using inverter. An insulated-gate bipolar transistor (IGBT) is considered as the inverter because of its high switching speed as shown in Fig. 7. A filter having with the elements value of $2mH$ and $15\mu F$ is set to address the issue related to the noises produced at the time of conversing DC to AC voltage. The regulator is developed for the regulation of SN load terminal voltage associated with solar-oriented MG plant by avoiding disturbance produced causing the nonlinear grid current Ig.

III. DESIGN SN VOLTAGE CONTROL WITH STABILITY ANALYSIS

The developed MR-FOPID controller is essentially made of two control loops namely inner-loop and outer-loop as depicted in Fig. 8. The outer control loop, known as the adaption loop, tunes the adaption gain using the MIT rule, while the inner loop is a well-tuned and stable FOPID control loop that improves the tracking control performance according to the direction of the reference model. By properly tuning the inner control loop parameters, the control error (error between the modified reference command regulated by the MIT and the plant output) can be set near to zero that confirms the controlled output effectively settle with the reference command. Accordingly, the main function of the outer-loop is to shape the reference command so as the model error value (mismatch output calculating from the reference and actual model) minimizes to zero. This action proves that the inner control loop follows the direction of the reference model which mainly regulates the action of the proposed modified controller. The details design of the proposed MR-FOPID controller can be done by separately designing of the FOPID, i.e., inner control loop and MRAC presented in the following section.

A. DESIGN OF MRAC

To achieve a desirable response, it is necessary to integrate a controller with the system to regulate the system parameters. In that sense, the proposed controller is developed as shown in Fig. 8 and integrated with the plant model T_G. The proposed MR-FOPID controller carries four basic building blocks and they are: reference model, fractional PID controller, adaptive mechanism, and nominal plant model. The reference model works here for generating the desired response. The signal coming from the plant is then compared with the reference model output and produces an error (model error). The adaptive mechanism uses this error to calculate the adaptation gain which resembles the shape of the modified system input for the control unit. The control unit, where a fractional order PID controller is merged with the adaptive mechanism, reduces the tracking error and ensures the optimal operation of the controller. An MIT principle is analyzed here to generate the adjustment parameter $\theta(m)$ that improves the tracking competency of the regulator unit.

The unintended operation of the inner control loop increases the control error that leads to large model error. The appearance of large model error increases the chance to show the unstable performance. Hence, the steady activity behind the demonstrating of MRAC relies upon the determination of the reference plant transfer function T_{Rm}. The parameters of the reference plant is picked such that the dynamic nature of the T_{Rm} is very like the actual model as so a low measure of error is delivered which can be resolved effectively by utilizing the MIT principle. An optimized function named gradient continuous descent optimization (GCDO) is implemented here to apply the MIT principle as,

$$j(\theta(m)) = \frac{1}{2} e_m^{*\,2}(\theta(m). \tag{9}$$

In (9), the error e_m^* indicates the model output mismatch obtained from the comparison of actual (y_{pm}) and reference (y_{rm}) model output. Then it is expressed as,

$$e_m^* = y_{pm} - y_{rm}. \tag{10}$$

Here in (10), the generated error can be solved by considering the parameter $\theta(m)$ obtained by applying the cost function in (9). This becomes possible when the considered objection function approaches to zero. This is secured by enabling the MIT principle which states that the variation of $\theta(m)$ directly changes in accordance with the change of the slop of j.

$$\frac{d\theta(m)}{dt} = -\kappa \frac{\delta j}{\delta \theta(m)} = -\kappa e_m^* \frac{\delta e_m^*}{\delta \theta(m)} sign(e_m^*), \tag{11}$$

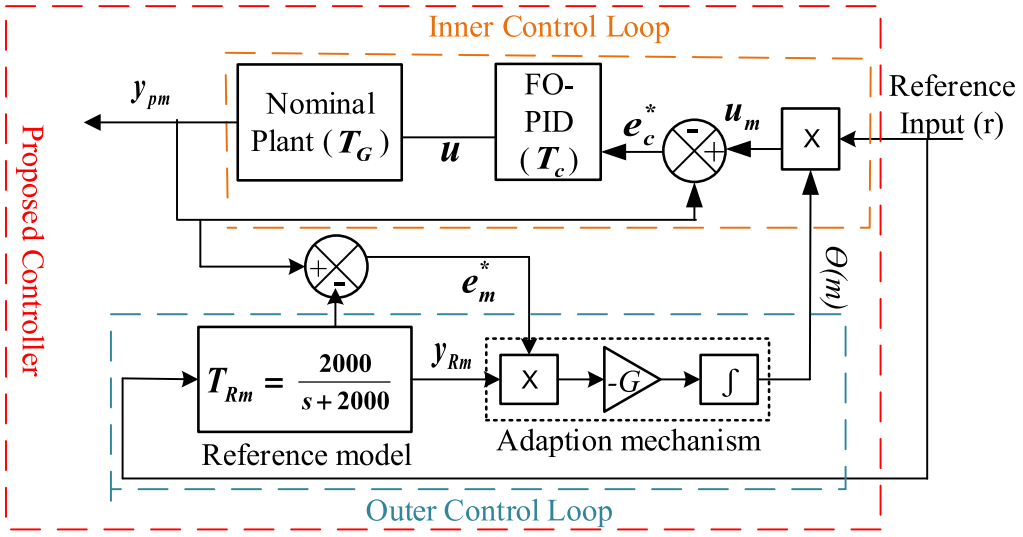

FIGURE 8. Graphical architecture of proposed adaptive MR-FOPID control framework.

where

$$sign(e_m^*) = \begin{cases} 1, & e_m^* > 0 \\ 0, & e_m^* = 0 \\ -1, & e_m^* < 0 \end{cases}$$

In (11), the element κ indicates the rate of learning which demands a proper tuning to track down the stability mapping of the objectives function exposed in (9). For this mapping, the reference plant is chosen to make error e_m^* more than zero. Then, we can express,

$$\frac{d\theta(m)}{dt} = -\kappa e_m^* \frac{\delta e_m^*}{\delta \theta(m)}, \tag{12}$$

Now, implementing the Laplace, Eq. (12) is noted as follows,

$$\theta(m) = -\kappa \frac{1}{s} e_m^* \frac{\delta e_m^*}{\delta \theta(m)}. \tag{13}$$

From the control structure presented in Fig. 8, we get for (10),

$$e_m^* = T_{Rm}\theta(m)r - T_{Rm}r = T_{Rm}r(\theta(m) - 1), \tag{14}$$

Applying partial derivative in reference to $\theta(m)$,

$$\frac{\delta e_m^*}{\delta \theta(m)} = T_{Rm}r. \tag{15}$$

Here, $r = \frac{y_{Rm}}{T_{Rm}}$. Using (15), we can describe in the form of,

$$\frac{\delta e_m^*}{\delta \theta(m)} = T_{Rm}\frac{y_{Rm}}{T_{Rm}} = T_{Rm}\frac{mT_{Rm}}{T_{Rm}} = T_{Rm}m. \tag{16}$$

Here, m indicates the user known parameters given in reference plant transfer function that prompts structure to make sensitivity error $\frac{\delta e_m^*}{\delta \theta(m)}$ and forms updated MIT principle. From (13),

$$\theta(m) = -\kappa \frac{1}{s} e_m^* y_{Rm} \tag{17}$$

TABLE 3. Parametric values for FO-PID controller.

Parameter	Value
K_p	250
K_i	5×10^5
λ	0.001
K_d	0.004
μ	1.99
γ	0.001

This term explains the updated adaption Gain $\theta(m)$ and it is contemplated as a limited quantity. It can be executed when the dynamic nature of the reference plant seems to be comparable with the actual plant transfer function i,e.,$y_{pm} \cong y_{Rm}$.

B. DESIGN OF FRACTIONAL ORDER PI$^\lambda$D$^\mu$

The fractional order differential equation describes the fractional order control systems. Fractional order (FO) calculus is an emerging mathematical technique that helps the derivative and integral terms to be in any arbitrary order. The mathematical study about the FO differentiator is as per the following:

$${}_\alpha D_t^\beta = \begin{cases} \frac{d^\beta}{dt^\beta}, & \mathrm{Re}(\beta) > 0 \\ 1, & \mathrm{Re}(\beta) = 0 \\ \int_a^t (d\tau)^{-\beta}, & \mathrm{Re}(\beta) < 0 \end{cases}$$

The term α in above inequality is a fixed value for the first condition and β explain the order of the integral. The definition noted below can be applied to measure the necessary fractional derivatives.

- Riemann-Liouville based FO derivatives definition:

$${}_\alpha D_t^\beta f(t) = \frac{1}{\Gamma(n-\alpha)}\frac{d^n}{dt^n}\int_a^t \frac{f(\tau)}{(t-\tau)^{\beta-n+1}} d\tau \tag{18}$$

where, $n > \beta > n-1$; $\Gamma(\bullet)$ is the Euler Gamma funciton.

FO-PID is developed by using the FOC where the given parameters (λ) and (μ) characterizes the integral and differential order for the framework. Considering the transfer function of the framework subsequent to adding the above two parameters can be formed as:

$$u(t) = K_p e(t) + K_i D^{-\lambda} e(t) + K_d D^{\mu} e(t) \tag{19}$$

Taking the Laplace transform of (19), the continuous transfer function of FO-PID is obtained as follows:

$$G(s) = K_p + \frac{K_i}{S^{\lambda}} + K_d S^{\mu} \tag{20}$$

From (20), it is observed that the FO-PID regulator becomes the traditional PID regulator when the parameters λ and μ is set to 1. The values of the controlling parameters used in this work are reported in Table 3. The given parameters are selected based on executing the trial and error approach and the best suitable control parameters are set to confirm the high tracking performance.

C. STABILITY ANALYSIS

The theoretical stability analysis of the proposed controller is carried out in this section. The investigation has been inferred by assuming the similar dynamic nature between the chosen reference plant and original plant. For this, we require to track down the practical state for e_m^* that demonstrates the necessary stability mapping for microgrid concerning with MR-FOPID control framework. The details derivation are presented as follows:

Since the inner control scheme is considered as well regulated stable loop, the model error $e_m^* = y_{Rm} - y_{pm} < \varepsilon \epsilon R$ obtained from the difference between inner-outer-loop confirms required stability state, i.e., bounded input bounded output (BIBO) for the proposed fixed MR-FOPID control structure.In such manner, we can investigate the fundamental state of e_m^* to set off zero. we can observe from (8) that the model error is possible set off 0 if the parameter $\theta(m)$ produced from the adaption mechanism becomes 1.

Theorem: For the stability of the proposed control framework, the closed-loop inner scheme needs to the stable, and can say to be stable when the e_m^* function becomes as,

$$e_m^* = -\frac{s^2+\omega^2}{\kappa\omega}(s + \frac{s}{T_c(s)T_G(s)}), \ \textit{when } s > 0$$

where the BIBO are stable. The error e_m^* converges to zero for the following equation,

$$\lim_{s\to 0^+} \frac{s^2+\omega^2}{\kappa\omega}(s^2 + \frac{s^2}{T_c(s)T_G(s)}) = 0$$

Proof: Let's think about the FOPID regulator is utilized as the inner control loop to diminish the time to set the common-state and extreme overshoot. This response guarantees the extended regulated performance of the system. A basic format of FOPID regulator is described in (20) associated with the plant $T_G(s)$ which builds a feed-forward inner control loop. Then, the inner-loop transfer function $T_{in}(s)$ can be expressed as,

$$T_{in}(s) = \frac{T_c(s)T_G(s)}{1 + T_c(s)T_G(s)} \tag{21}$$

From (11), we can derived,

$$e_m^* = -\frac{s\theta(m)}{\kappa y_{Rm}} \tag{22}$$

It seems from Fig. 8 that the outcome of the selected reference plant $y_{Rm} = T_{Rm}r$. For the stability mapping, the responses of the framework considers as a step output when the closed-loop framework reaches to the set-point slowly. Therefore, the output of the reference model can be written as $y_{Rm} = T_{Rm}\frac{\omega}{s^2+\omega^2}$. Here, the term $r = \frac{\omega}{s^2+\omega^2}$ is the Laplace transform of given reference input. From (22),

$$e_m^* = -\frac{s\theta(m)}{\kappa T_{Rm}} \tag{23}$$

Here, the error e_m^* becomes zero when $\theta(m) = 1$ is assumed when $T_{Rm} = T_{in}$. Using (23), we get,

$$e_m^* = -\frac{s(s^2+\omega^2)}{\kappa\omega T_{in}} \tag{24}$$

In (25), the element T_{in} is continuously offered the stable response by using the optimal FOPID regulator parameters. Now using (21) in (25), we can obtain as follows,

$$\begin{aligned} e_m^* &= -\frac{s(s^2+\omega^2)}{\kappa\omega}(\frac{1 + T_c(s)T_G(s)}{T_c(s)T_G(s)}) \\ &= -\frac{s(s^2+\omega^2)}{\kappa\omega}(1 + \frac{1}{T_c(s)T_G(s)}) \\ &= -\frac{s^2+\omega^2}{\kappa\omega}(s + \frac{s}{T_c(s)T_G(s)}) \end{aligned}$$

which is appeared to be stable. Therefore, the performance of closed-loop inner control scheme is bounded for given reference signal. Thus, applying final value conditions we can write,

$$\lim_{s\to 0^+} se_m^* = 0 \tag{25}$$

Finally, we can derive the following conditions

$$\lim_{s\to 0^+} \frac{s^2+\omega^2}{\kappa\omega}(s^2 + \frac{s^2}{T_c(s)T_G(s)}) = 0$$

TABLE 4. Various industrial loads rating considered to measure the controller performance.

Single-phase Industrial Loads (KW)			
Consumer	Harmonic	Asynchronous machine	Dynamic
2.26	4.325	4.4	2.4
Three-phase Industrial Loads (KW)			
Consumer	Balance	Unbalance	
3	4.13	3.25	

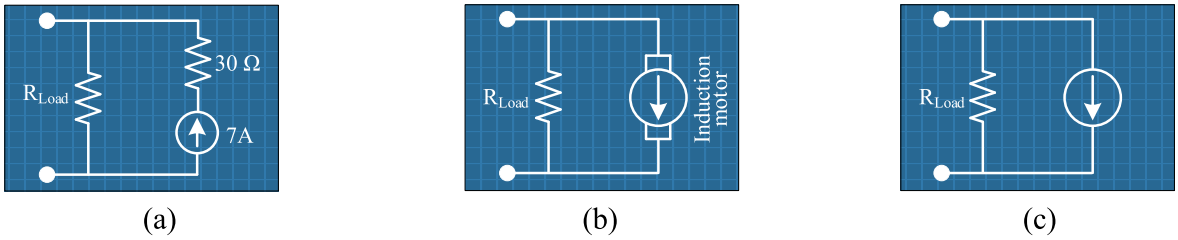

FIGURE 9. Single-phase industrial loads (a) harmonic load (b) asynchronous machine load and (c) dynamic load.

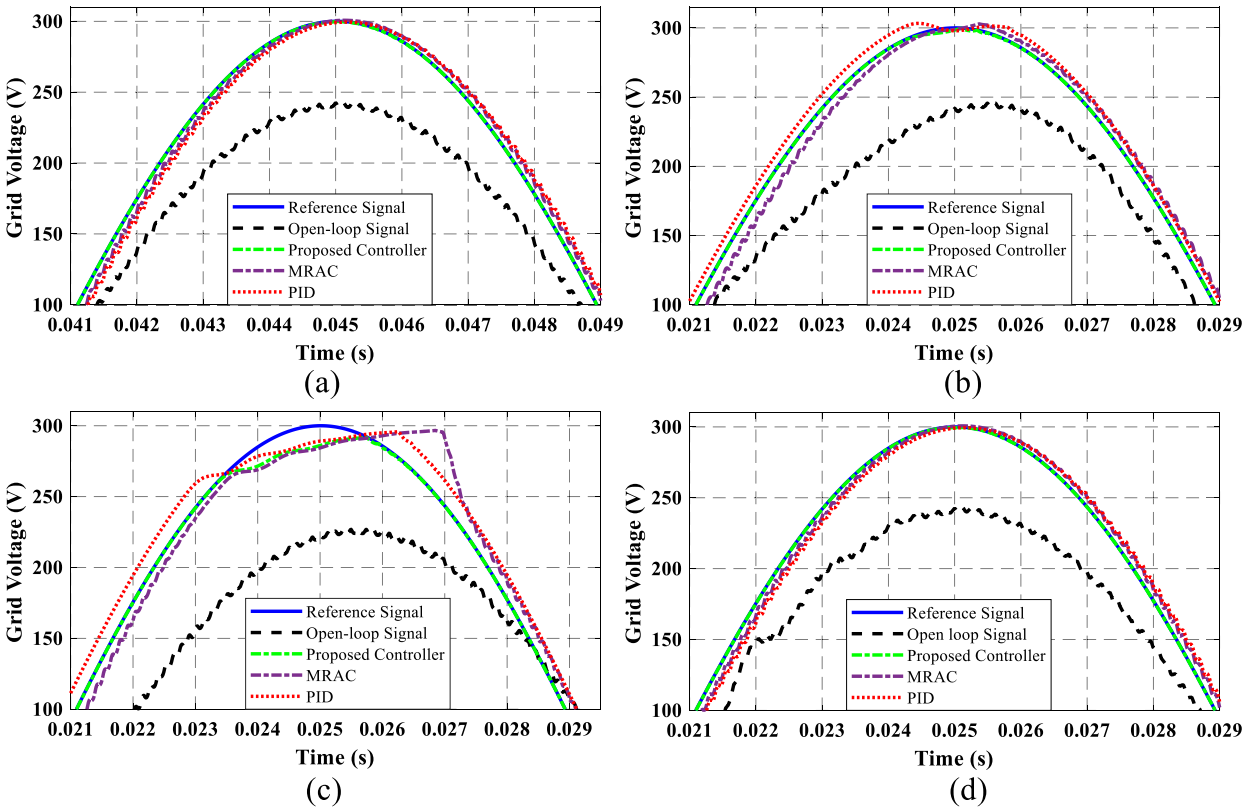

FIGURE 10. Comparison of secondary network/grid voltage tracking using the MR-FOPID controller, MRAC, and PID against (a) consumer load (b) harmonic load (c) asynchronous machine load and (d) dynamic load.

IV. PERFORMANCE EVALUATION

The control competency of the proposed ancillary voltage control framework is analyzed by using the variation of industrial loads. The analysis is carried out for two SNs associated with PV based MG system and the simulations are done by MATLAB R2016b software. The operation of these SNs is studied with two different frequency conditions (50 Hz for single-phase SN and 60 Hz for three-phase SN) to measure the high efficacy of the proposed MR-FOPID regulator. The detail results of this analysis is discussed in the following section.

A. TRACKING PERFORMANCE AGAINST VARIOUS SINGLE PHASE INDUSTRIAL LOADS

In this section, the controller performance against various single-phase loads presented in Fig. 9 are evaluated. Different single-phase loads are designed and their ratings are reported in Table 4. The efficacy of the MR-FOPID control framework over the industrial loads presented in Fig. 9 is described as follows:

For the single-phase consumer load, the load and line resistance are chosen as 40Ω and 0.45Ω, respectively. The controller behaviour under the running of single phase consumer load is recorded and shown in Fig. 10(a). From the result, it is noted that the fixed control framework MR-FOPID offers better tracking response for the voltage of the secondary network or grid.

A load like television, computer, printer, fluorescent light etc are considered as harmonic load that produces more harmonic during their operation at high frequency region. For the harmonic load, a $7A - 150Hz$ current source is used and a resistance containing the value of 30Ω is fed with the current

TABLE 5. Percentage of tracking error voltage (RMS) comparison among the different controllers for various loads.

Name of Load	**Proposed controller**	MRAC	PID [20]	LQR [22]	MPC [25]	RC [5]
Consumer	**0.21**	0.29	0.45	7.38	0.69	0.97
Harmonic	**0.65**	0.85	3.13	21.1	7.13	3.43
Asynchronous machine	**1.31**	2.79	4.88	73.8	17.27	13.34
Dynamic	**0.25**	0.38	0.76	1.33	0.65	0.58

source shown in Fig. 9(a) in following the series manner. The effectiveness of the MR-FOPID controller over the harmonic load is depicted in Fig. 10(b). Here, it is observed that the voltage without concerning the controller is unable to deal with tracking response with the reference input voltage, while the system response concerning with controller can easily track the reference signal. Three types of controllers are used to form the closed-loop system. Among them, the reconciliation of MR-FOPID control structure with the framework gives a better regulatory response in terms tracking voltage for harmonic load.

An electric motor named induction motor is used as the asynchronous machine load which might motivation to corrupt the framework response due to their dynamic nature. The efficacy of the fixed MR-FOPID regulator is studied with the integration of an asynchronous load into the SN premises. A dq stator with zero steady-state condition is considered for the modelling of this load reported in Fig. 9(b) and is connected to the SN in parallel manner. When the machine is in running condition, the active and reactive power continuously changes. This alteration in power is the reason of poor performance of the MG. This poor performance can be reduced by the inclusion of the proposed MR-FOPID controller with the SN system. The controller lessen the variation in power by reducing the voltage variation. From Fig. 10(c), it is reported that the proposed control method gives high voltage tracking against the asynchronous machine load and ensures the reliable performance of the system.

In order to measure the high performance of the MR-FOPID controller, a single-phase dynamic load is integrated with the SN system. A current source having with active power of $50MW$ and reactive power of $25MW$ is used for designing the dynamic load shown in Fig. 9(c). The variation in voltage waveform alters the active and reactive power of the system that affects the system performance immensely. Effectiveness of the proposed MR-FOPID controller under this load is measured and the associated results are figured out in Fig. 10(d), from which it is proven that the proposed MR-FOPID controller secures the higher voltage tracking performance for the sound operation of the SN.

The performance of the proposed controller is further tested through the measuring of the total harmonic distortion (THD) for each single-phase load voltage presented in this paper. The voltage THD for four loads are illustrated in Fig. 11 where it is seen that the proposed MR-FOPID controller provides 1.78%, 1.82%, 3.05% and 1.62% THD for each load respectively. The quantitative results seen from Fig. 11 indicates that the controller can improve the voltage quality of the MG.

1) COMPARATIVE PERFORMANCES

To confirm the high performance of the MR-FOPID controller, its performance is compared with the model reference adaptive control (MRAC) and PID controller separately. The reason behind this comparison is to ensure the improved tracking performance of the proposed modified controller as compared to its component used to make the modified controller. Here, the MRAC and PID controller is designed based on the same problem statement. The comparative performance of MR-FOPID controller is shown in Fig. 10 and the quantitative measurements are presented in Table 5. From these results, it is seen that the proposed controller is capable of showing better voltage tracking as compared to its component controller. A comparison between the proposed MR-FOPID controller and other methods from literature is also carried out in Table 5 in terms of the percentage of tracking error voltage for various load dynamics. It is concluded that the proposed controller not only allows improved tracking performance as compared to the same dimensional controller but also provides a competitive tracking performance along with the existing LQR, MPC, and resonant controller (RC).

B. PERFORMANCE ENHANCEMENT WITH MULTI VARIABLE SN (MVSN)

1) MODELING OF MVSN

To ensure the high effectiveness of the MR-FOPID controller, the efficacy is tested by integrating the MVSN in Fig. 1 in the place of single-phase SN and operated it with the input voltage refereed in Fig. 6(c). The schematic of an MVSN is exposed in Fig. 12 made by using a six pulses IGBT as the VSI, transformer to step-up the supplied voltage, filter to suppress noise, and loads. The motivation behind the consideration of IGBT is to invert the regulated common bus voltage so as the several number of three-phase industrial loads used in real-time can be integrated into the MVSN premises. The studied loads are associated with MVSN in a parallel way to notice the dynamic nature and LC filter is associated in series to reduce the oscillation produced during the switching of voltage. The capacitor C_2 in LC filter mainly focuses to reduce the load harmonics. The dynamics of multi-variable secondary network system is given as follows,

Consider a MVSDN presented in Fig. 12 which is balanced and symmetry in its initial operating point. From Fig. 12,

$$\frac{d\tilde{I}_{s,abc}}{dt} = -\frac{R_2}{L_2}\tilde{I}_{s,abc} + \frac{1}{L_2}\tilde{V}_{s,abc} - \frac{1}{L_2}\tilde{V}_{2,abc} \qquad (26)$$

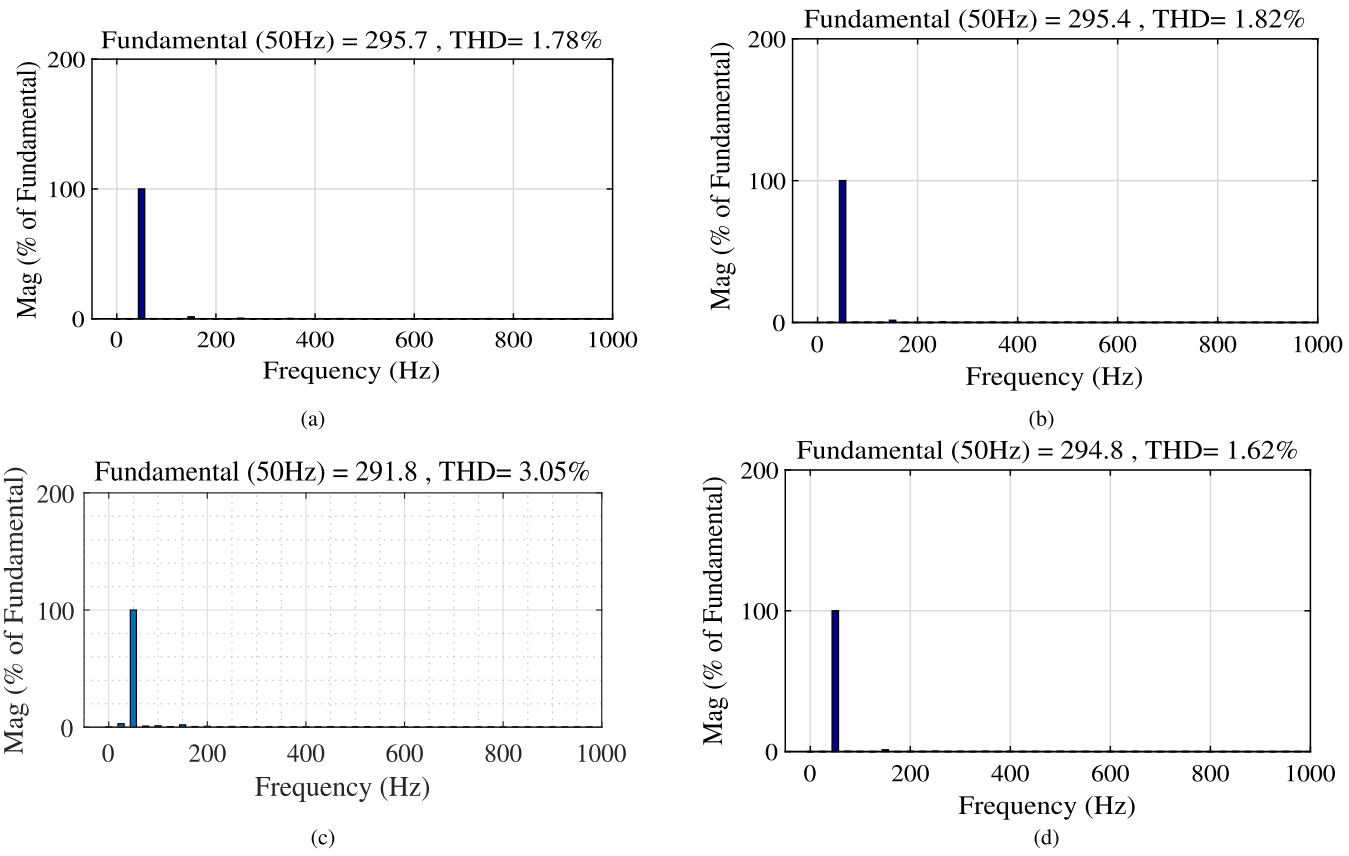

FIGURE 11. Closed-loop voltage THD using proposed controller under the operation of (a) consumer load, (b) harmonic, (c) asynchronous machine load and (d) dynamic load.

and

$$\frac{d\tilde{V}_{2,abc}}{dt} = \frac{1}{C_2}\tilde{I}_{s,abc} \tag{27}$$

Eq. (26) and (27) can be expressed in terms of dq reference form so the system can be regulated by enabling the single fixed structured controller.

$$\frac{d\tilde{I}_{s,dq}}{dt} = -j\omega_0\tilde{I}_{s,dq} - \frac{R_2}{L_2}\tilde{I}_{s,dq} + \frac{1}{L_2}\tilde{V}_{s,dq} - \frac{1}{L_2}\tilde{V}_{2,dq} \tag{28}$$

and

$$\frac{d\tilde{V}_{2,dq}}{dt} = -j\omega_0\tilde{V}_{2,dq} + \frac{1}{C_2}\tilde{I}_{s,dq} \tag{29}$$

From (28) and (29), the control model for MVSN can be manifested as, $A_p = \begin{bmatrix} 0 & \omega_0 & \frac{1}{C_2} & 0 \\ -\omega_0 & 0 & 0 & \frac{1}{C_2} \\ -\frac{1}{L_2} & 0 & -\frac{R_2}{L_2} & \omega_0 \\ 0 & -\frac{1}{L_2} & \omega_0 & -\frac{R_2}{L_2} \end{bmatrix}$, $B_p = \begin{bmatrix} 0 & 0 \\ 0 & 0 \\ \frac{1}{L_2} & 0 \\ 0 & \frac{1}{L_2} \end{bmatrix}$, $C_p = \begin{bmatrix} 1 & 0 & 0 & 0 \\ 0 & 1 & 0 & 0 \end{bmatrix}$ and $D_p = 0$

where $x = \left[\tilde{V}_{2,d}\ \tilde{V}_{2,q}\ \tilde{I}_{s,d}\ \tilde{I}_{s,q}\right]^T$, $u = \left[\tilde{V}_{2,d}\ \tilde{V}_{2,q}\right]^T$ and $y = \left[\tilde{V}_{2,d}\ \tilde{V}_{2,q}\right]$. The parametric values of MVSN is given in Table 6.

TABLE 6. Parametric values of three-phase secondary-network microgrid.

Description	Value
Voltage from DC bus (V_{dc})	2000 V
VSI voltage (V_T)	500V (1 pu)
Transformer ratio (Y/Δ)	0.6/13.8
Carrier frequency (f_{sw})	1980 Hz
System frequency (f_0)	60 Hz
Filter resistance (R_2)	1.5$m\Omega$
Filter inductance (L_2)	100 μH
Filter capacitance (C_2)	100 μF
Consumer load parameters	R= 4.33 Ω, L= 100 mH and C= 1 pF

2) TRACKING PERFORMANCE AGAINST VARIOUS THREE PHASE INDUSTRIAL LOADS

The role of the designed MR-FOPID control framework for the regulation of a multi-variable SN system is explored here by executing a group of experiments. The subsystem

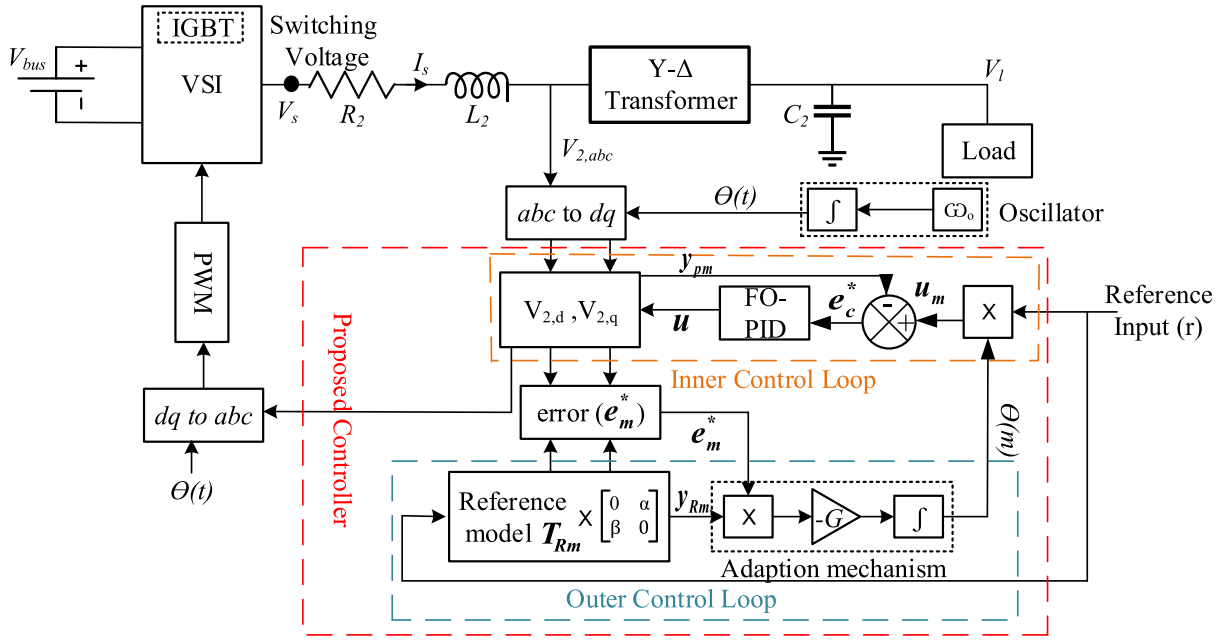

FIGURE 12. Closed-loop control diagram of multi-variable secondary network with proposed model reference modified adaptive fractional order PID controller.

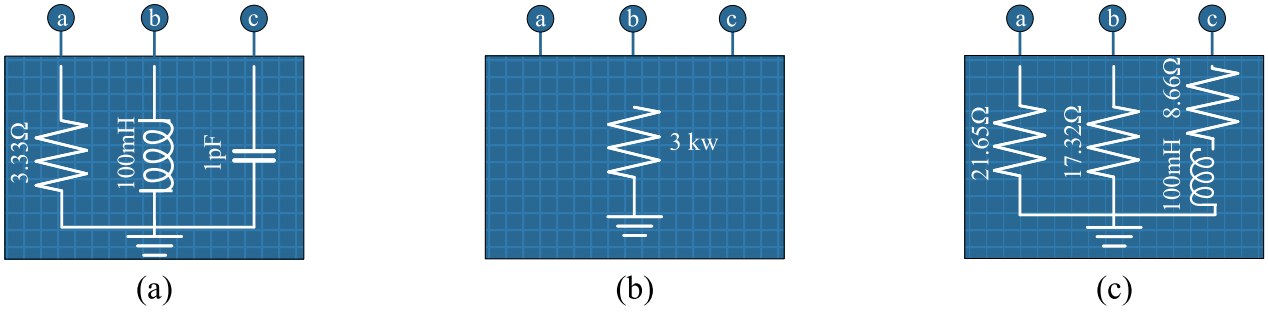

FIGURE 13. Three phase (a) consumer load (b) balance load (c) unbalance load.

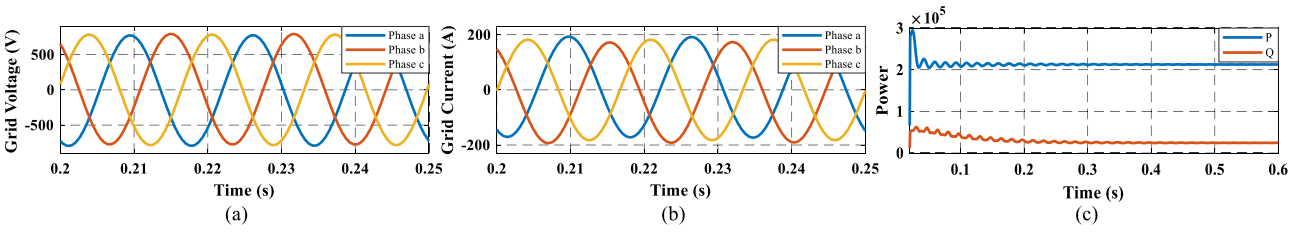

FIGURE 14. Performance of multi-variable SN without MR-FOPID in terms of (a) voltage, (b) current, (c) power under the analysis of consumer load.

enlargement into the considered microgrid model may cause to build the SN protection issue more complex. Every one of the subsystems are modelled with the at least two energy ingested sources that increase the regulating parameters. These expanded regulating parameters make the multi-variable SN more difficult. For this, several multi-variable industrial loads are incorporated into the MVSN premises in accordance with the Fig. 13 and Table 4, and the role of MR-FOPID framework are observed in the next three parts.

A schematic for the three phase consumer load is presented in Fig. 13(a) and the performance of the controller against this load is investigated. The open-loop response of the SN system is shown in Fig. 14(a), (b), and (c) in terms of voltage, current, and power, respectively. The proposed MR-FOPID controller having with same design parameters is applied against this

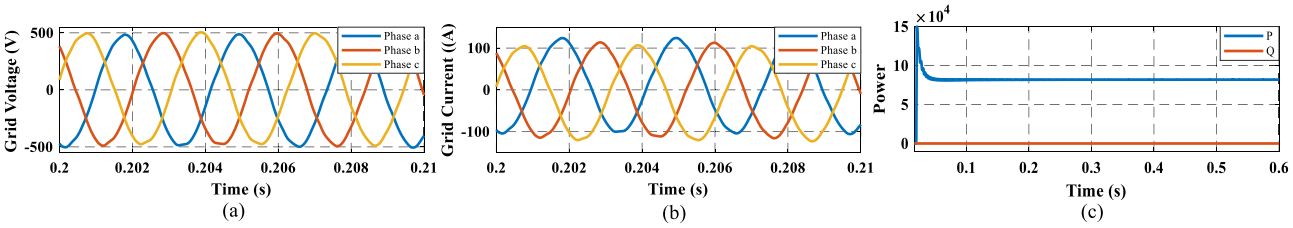

FIGURE 15. Performance of multi-variable SN with MR-FOPID in terms of (a) voltage, (b) current, (c) power under the analysis of consumer load.

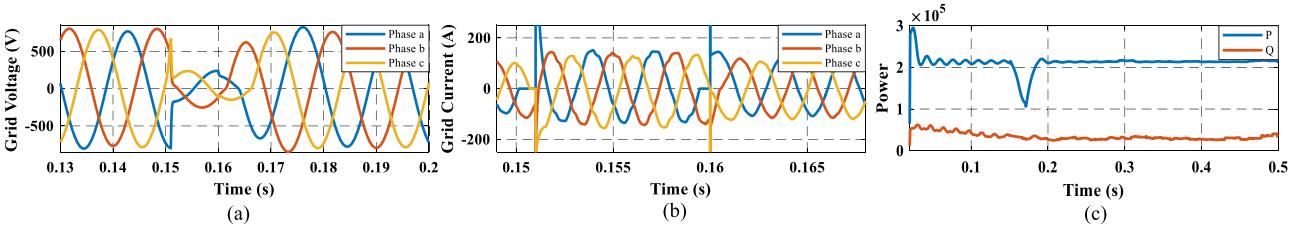

FIGURE 16. Performance of multi-variable SN without MR-FOPID in terms of (a) voltage, (b) current, (c) power under the analysis of balance load.

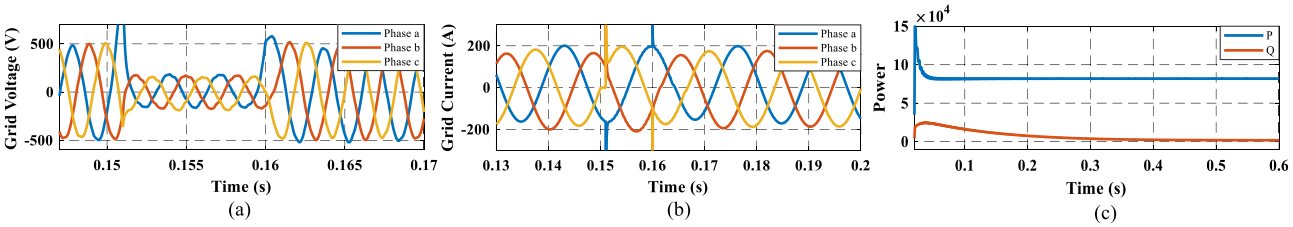

FIGURE 17. Performance of multi-variable SN with MR-FOPID in terms of (a) voltage, (b) current, (c) power under the analysis of balance load.

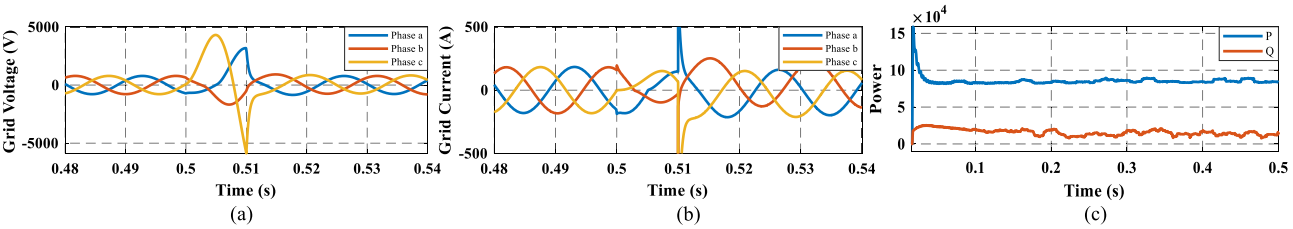

FIGURE 18. Performance of multi-variable SN without MR-FOPID in terms of (a) voltage, (b) current, (c) power under the analysis of un-balance load.

load and control responses are presented in Fig. 15(a) to (c). From the simulated results, it is seen that the controller provides an expected control performance for the voltage, current, and power against a three-phase consumer load.

A three-phase balance load is shown in Fig. 13(b) and the performance of MR-FOPID framework over this load is presented in this section. The modeling of the load consists of a resistive load of $3KW$ active power and $60V$ of phase-to-phase voltage, and the load is applied to the system from $t = 0.15s$ to $t = 0.16s$. In Fig. 16(a)-(c), open-loop voltage, current, and power of the multi-variable SN associated with three-phase balance load is demonstrated. The control parameters are maintained by using the proposed controller and its performances are illustrated in Fig. 17(a), (b), and (c), respectively. The results ensure that the controller gives desired regulatory performance on the three phase parameters and takes a bit amount of time to reach the transient response for power signal.

The diagram of a three-phase unbalance load is depicted in Fig. 13(c) and used in MVSN terminal after $t = 0.5s$. The load is constructed by three resistors having the value of $R_a = 21.65\Omega$, $R_b = 17.32\Omega$, and $R_c = 8.66\Omega$, respectively and an inductor with the value of $L_c = 100mH$. As the load is included to the system, its instantaneous voltage becomes imbalanced and the open-loop response for voltage, current, and power for this load is given in Fig. 18(a), (b), and (c), respectively. The response of the proposed controller against this condition is presented in Fig. 19(a) to (c), respectively

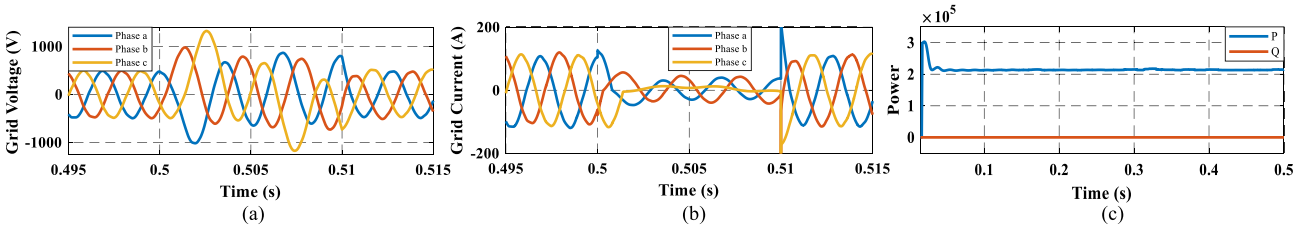

FIGURE 19. Performance of multi-variable SN with MR-FOPID in terms of (a) voltage, (b) current, (c) power under the analysis of un-balance load.

that proves the controller is capable of showing control performance for the three-phase unbalance load.

V. CONCLUSION

This study presents the recognized ancillary control solution for the use of renewable energy sources such as PV sources against the number of industrial loads. A hybrid microgrid (HMG) system associated with multiple inverter-based secondary networks is studied first to formulate the challenges for the operation of various industrial loads. The studied HMG contains the PV and utility AC grid source which acts as the prime mover for driven the industrial loads. A DC bus technology is used to integrate all of the sources in a single network so as the output voltage can be fed directly to the industrial loads via the inverter of the SNs. For the balance operation of the SNs, the output of the DC bus needs to be stable over the variation of temperature, irradiance and consumer demand.

This paper carries the design of an intelligent adaptive controller (IAC) through the combination of an ANN and a PI controller. The validation of the IAC is studied by varying the consumer demand and the meteorological factors of the PV source. Results obtain from this study confirms that the proposed IAC has the ability to provide the stable input voltage for the SN. The operation of the SNs is subjected to the variation load dynamics that may change the operating environment and confirms the low tracking performance. This paper also carries the design of a novel MR-FOPID controller to control the inverters associated with SNs and enabling them to provide improved tracking performance. The tracking assessment of the MR-FOPID controller is tested by changing the loads in the SNs terminal. Results reveal that the controller shows high performance as compared to other controllers and offers low tracking error with a value of 0.21%, 0.65%, 1.31% and 0.25% for the single-phase consumer, harmonic, asynchronous machine, and dynamic load respectively. The future work of this study is to develop a learning base tracking controller and implement it real-life microgrid system.

REFERENCES

[1] D. Datta, S. R. Fahim, S. K. Sarker, S. M. Muyeen, M. R. I. Sheikh, and S. K. Das, "A robust control method for damping and tracking of secondary network voltage of a PV based hybrid AC/DC microgrid," *Frontiers Energy Res.*, vol. 7, Nov. 2020, Art. no. 580840.

[2] M. T. Rizi and H. Eliasi, "Nonsingular terminal sliding mode controller for voltage and current control of an islanded microgrid," *Electr. Power Syst. Res.*, vol. 185, Aug. 2020, Art. no. 106354.

[3] F. R. Badal, P. Das, S. K. Sarker, and S. K. Das, "A survey on control issues in renewable energy integration and microgrid," *Protection Control Modern Power Syst.*, vol. 4, no. 1, p. 8, Dec. 2019.

[4] M. Babazadeh and H. Karimi, "A robust two-degree-of-freedom control strategy for an islanded microgrid," *IEEE Trans. Power Del.*, vol. 28, no. 3, pp. 1339–1347, Jul. 2013.

[5] S. K. Sarkar, M. H. K. Roni, D. Datta, S. K. Das, and H. R. Pota, "Improved design of high-performance controller for voltage control of islanded microgrid," *IEEE Syst. J.*, vol. 13, no. 2, pp. 1786–1795, Jun. 2018.

[6] A. Kumar, A. R. Singh, Y. Deng, X. He, P. Kumar, and R. C. Bansal, "A novel methodological framework for the design of sustainable rural microgrid for developing nations," *IEEE Access*, vol. 6, pp. 24925–24951, 2018.

[7] M. Armin, M. Rahman, M. M. Rahman, S. K. Sarker, S. K. Das, M. R. Islam, A. Z. Kouzani, and M. A. P. Mahmud, "Robust extended H_∞ control strategy using linear matrix inequality approach for islanded microgrid," *IEEE Access*, vol. 8, pp. 135883–135896, 2020.

[8] K. T. Tan, B. Sivaneasan, X. Y. Peng, and P. L. So, "Control and operation of a DC grid-based wind power generation system in a microgrid," *IEEE Trans. Energy Convers.*, vol. 31, no. 2, pp. 496–505, Jun. 2015.

[9] H. A. Gabbar and A. A. Abdelsalam, "Microgrid energy management in grid-connected and islanding modes based on SVC," *Energy Convers. Manage.*, vol. 86, pp. 964–972, Oct. 2014.

[10] S. K. Sarkar, F. R. Badal, and S. K. Das, "A comparative study of high performance robust PID controller for grid voltage control of islanded microgrid," *Int. J. Dyn. Control*, vol. 6, no. 3, pp. 1207–1217, Sep. 2018.

[11] H. R. Baghaee, A. Parizad, P. Siano, M. Shafie-khah, G. J. Osório, and J. P. Catalão, "Robust probabilistic load flow in microgrids considering wind generation, photovoltaics and plug-in hybrid electric vehicles," in *Proc. IEEE 16th Int. Conf. Ind. Inform. (INDIN)*, Jul. 2018, pp. 978–983.

[12] M. Marzband, E. Yousefnejad, and A. Sumper, "Real time experimental implementation of optimum energy management system in standalone microgrid by using multi-layer ant colony optimization," *Int. J. Elect. Power Energy Syst.*, vol. 75, pp. 265–274, Feb. 2016.

[13] M. A. Mahmud, M. J. Hossain, H. R. Pota, and A. M. T. Oo, "Robust nonlinear distributed controller design for active and reactive power sharing in islanded microgrids," *IEEE Trans. Energy Convers.*, vol. 29, no. 4, pp. 893–903, Dec. 2014.

[14] R. Viral and D. K. Khatod, "An analytical approach for sizing and siting of DGs in balanced radial distribution networks for loss minimization," *Int. J. Electr. Power Energy Syst.*, vol. 67, pp. 191–201, May 2015.

[15] S. Augustine, M. K. Mishra, and N. Lakshminarasamma, "Adaptive droop control strategy for load sharing and circulating current minimization in low-voltage standalone DC microgrid," *IEEE Trans. Sustain. Energy*, vol. 6, no. 1, pp. 132–141, Jan. 2014.

[16] M. Mokhtar, M. I. Marei, and A. A. El-Sattar, "An adaptive droop control scheme for DC microgrids integrating sliding mode voltage and current controlled boost converters," *IEEE Trans. Smart Grid*, vol. 10, no. 2, pp. 1685–1693, Mar. 2017.

[17] S. K. Das, D. Datta, S. Sarker, S. R. Fahim, M. R. I. Sheikh, and F. R. Badal, "Improved voltage oscillation damping and tracking of subgrid of a hybrid AC/DC microgrid using robust integral linear quadratic Gaussian control," in *Proc. 2nd Int. Conf. Smart Power Internet Energy Syst. (SPIES)*, Sep. 2020, pp. 299–304.

[18] A. B. Siddique, S. Munsi, S. K. Sarkar, and S. K. Das, "Model reference modified adaptive PID controller design for voltage and current control of islanded microgrid," in *Proc. 4th Int. Conf. Electr. Eng. Inf. Commun. Technol. (iCEEiCT)*, Sep. 2018, pp. 130–135.

[19] S. H. Sikder, M. M. Rahman, S. K. Sarkar, S. K. Das, M. A. Rahman, and M. Akter, "Implementation of nelder-mead optimization in designing fractional order pid controller for controllingvoltageof islanded microgrid," in *Proc. Int. Conf. Advancement Electr. Electron. Eng. (ICAEEE)*, Nov. 2018, pp. 1–4.
[20] M. Armin, P. N. Roy, S. K. Sarkar, and S. K. Das, "LMI-based robust PID controller design for voltage control of islanded microgrid," *Asian J. Control*, vol. 20, no. 5, pp. 2014–2025, 2018.
[21] M. Ghafouri, U. Karaagac, H. Karimi, S. Jensen, J. Mahseredjian, and S. O. Faried, "An LQR controller for damping of subsynchronous interaction in DFIG-based wind farms," *IEEE Trans. Power Syst.*, vol. 32, no. 6, pp. 4934–4942, Nov. 2017.
[22] M. S. Munsi, A. B. Siddique, S. K. Das, S. K. Paul, M. R. Islam, and M. A. Moni, "A novel blended state estimated adaptive controller for voltage and current control of microgrid against unknown noise," *IEEE Access*, vol. 7, pp. 161975–161995, 2019.
[23] S. K. Sarker, F. R. Badal, P. Das, and S. K. Das, "Multivariable integral linear quadratic Gaussian robust control of islanded microgrid to mitigate voltage oscillation for improving transient response," *Asian J. Control*, vol. 21, no. 4, pp. 2114–2125, 2019.
[24] C. A. Hans, P. Braun, J. Raisch, L. Grüne, and C. Reincke-Collon, "Hierarchical distributed model predictive control of interconnected microgrids," *IEEE Trans. Sustain. Energy*, vol. 10, no. 1, pp. 407–416, Jan. 2018.
[25] S. K. Sarkar, F. R. Badal, S. K. Das, and Y. Miao, "Discrete time model predictive controller design for voltage control of an islanded microgrid," in *Proc. 3rd Int. Conf. Electr. Inf. Commun. Technol. (EICT)*, Dec. 2017, pp. 1–6.
[26] J. Hu, Y. Xu, K. W. Cheng, and J. M. Guerrero, "A model predictive control strategy of PV-battery microgrid under variable power generations and load conditions," *Appl. Energy*, vol. 221, pp. 195–203, Jul. 2018.
[27] M. Liserre, R. Teodorescu, and F. Blaabjerg, "Multiple harmonics control for three-phase grid converter systems with the use of PI-RES current controller in a rotating frame," *IEEE Trans. Power Electron.*, vol. 21, no. 3, pp. 836–841, May 2006.
[28] U. K. Kalla, B. Singh, S. S. Murthy, C. Jain, and K. Kant, "Adaptive sliding mode control of standalone single-phase microgrid using hydro, wind, and solar PV array-based generation," *IEEE Trans. Smart Grid*, vol. 9, no. 6, pp. 6806–6814, Nov. 2017.
[29] P. Li and Z.-Q. Zheng, "Robust adaptive second-order sliding-mode control with fast transient performance," *IET Control Theory Appl.*, vol. 6, no. 2, pp. 305–312, Jan. 2012.
[30] X. Huang, K. Wang, J. Qiu, L. Hang, G. Li, and X. Wang, "Decentralized control of multi-parallel grid-forming DGs in islanded microgrids for enhanced transient performance," *IEEE Access*, vol. 7, pp. 17958–17968, 2019.
[31] M. F. Firuzi, A. Roosta, and M. Gitizadeh, "Stability analysis and decentralized control of inverter-based AC microgrid," *Protection Control Mod. Power Syst.*, vol. 4, no. 6, pp. 1–24, 2019.
[32] L. Sedghi, M. Emam, A. Fakharian, and M. Savaghebi, "Decentralized control of an islanded microgrid based on offline model reference adaptive control," *J. Renew. Sustain. Energy*, vol. 10, no. 6, Nov. 2018, Art. no. 065301.
[33] Q. Shafiee, S. Member, J. M. Guerrero, S. Member, and J. C. Vasquez, "Distributed secondary control for islanded microgrids—A novel approach," *IEEE Trans. Power Electron.*, vol. 29, no. 2, pp. 1018–1031, Feb. 2013.
[34] T. Mahto and V. Mukherjee, "A novel scaling factor based fuzzy logic controller for frequency control of an isolated hybrid power system," *Energy*, vol. 130, pp. 339–350, Jul. 2017.
[35] S. Zhang, Y. Mishra, and M. Shahidehpour, "Fuzzy-logic based frequency controller for wind farms augmented with energy storage systems," *IEEE Trans. Power Syst.*, vol. 31, no. 2, pp. 1595–1603, Mar. 2015.
[36] M. Hasan, R. Sultana, S. K. Sarker, M. M. Rashid, S. K. Das, and M. R. I. Sheikh, "Improved secondary network voltage control with stability analysis for PV based microgrid," in *Proc. 2nd Int. Conf. Robot., Electr. Signal Process. Techn. (ICREST)*, Jan. 2021, pp. 248–252.
[37] J.-S. Ko, J.-H. Huh, and J.-C. Kim, "Overview of maximum power point tracking methods for PV system in micro grid," *Electronics*, vol. 9, no. 5, p. 816, May 2020.
[38] S. A. Mohamed and M. Abd El Sattar, "A comparative study of P&O and INC maximum power point tracking techniques for grid-connected PV systems," *Social Netw. Appl. Sci.*, vol. 1, no. 2, p. 174, Feb. 2019.
[39] S. R. Fahim, Y. Sarker, O. K. Islam, S. K. Sarker, M. F. Ishraque, and S. K. Das, "An intelligent approach of fault classification and localization of a power transmission line," in *Proc. IEEE Int. Conf. Power, Electr., Electron. Ind. Appl. (PEEIACON)*, Nov. 2019, pp. 53–56.
[40] Z. Farooq, T. Zaman, M. A. Khan, S. M. Muyeen, and A. Ibeas, "Artificial neural network based adaptive control of single phase dual active bridge with finite time disturbance compensation," *IEEE Access*, vol. 7, pp. 112229–112239, 2019.
[41] Y. Li and Y. Yuan, "Convergence analysis of two-layer neural networks with relu activation," in *Pro. Adv. Neural Inf. Process. Syst.*, 2017, pp. 597–607.
[42] D. P. Kingma and J. Ba, "Adam: A method for stochastic optimization," 2014, *arXiv:1412.6980*. [Online]. Available: http://arxiv.org/abs/1412.6980

SUBRATA K. SARKER was born in Bangladesh, in 1996. He received the Bachelor of Science degree in mechatronics engineering from the Rajshahi University of Engineering and Technology (RUET), Rajshahi, Bangladesh. He is currently working as a Lecturer with the RUET. Before joining at RUET, he worked as a Lecturer with the Electrical and Electronic Engineering Department, Varendra University, Rajshahi. He has been worked as an active reviewer for many prestigious journals and conferences. He has published more than 30 high-impact journal articles and 40 international conferences in his specialist field. His research interests include control theory and applications, electro-mechanical systems, robotics, mechatronics systems, artificial intelligence, and power systems.

SHAHRIAR RAHMAN FAHIM (Member, IEEE) received the B.Sc. degree in electrical and electronic engineering from the Rajshahi University of Engineering and Technology. His specialties in power transmission systems are fault detection, fault classification, fault location, power-quality event analysis, computer relaying, solar generation systems, and smart-grid systems. His research interests include diverse and cover human–machine interaction (HMI) and artificial intelligence. Currently, his research focuses on data-driven predictive maintenance, detection, diagnostics and prognostics, and application of machine-learning techniques in signal processing.

NILOY SARKER (Member, IEEE) was born in Bangladesh, in 1999. He received the Bachelor of Science degree in electrical and electronic engineering from American International University-Bangladesh. He is passionate about innovative research in power transmission systems, fault detection, fault classification, and fault location. His current research interests include solar generation systems and smart grid systems.

KAZI ZAKARIA TAYEF was born in December 1999. He is currently a Student of electrical and electronics engineering at American International University-Bangladesh (AIUB), Dhaka, Bangladesh. His research interests include power systems, renewable energy, and robotics. His research focuses on image processing with CNN method.

ABU BAKAR SIDDIQUE was born in Chandpur, Bangladesh. He received the B.Sc. degree from the Department of Mechatronics Engineering, Rajshahi University of Engineering and Technology (RUET), Rajshahi, Bangladesh, in 2019. He is currently pursuing the M.A.Sc. degree in nuclear engineering with Ontario Tech University, Canada. His research interests include nuclear power plant, small and micro modular reactor, fast charging station connected to NPP and their control strategies, renewable energy systems, and intelligent control systems.

DRISTI DATTA was born in October 1992. He received the B.Sc. and M.Sc. degrees from the Rajshahi University of Engineering and Technology, in 2014 and 2019, respectively. He is currently working as a Senior Lecturer with the Department of EEE, Uttara University, Dhaka, Bangladesh. Before that, he worked as an Assistant Professor with the Department of EEE, Varendra University, Rajshahi, Bangladesh. His research interests include power system control and stability, smart grid, microgrid, and the IoT-based power plant.

M. A. PARVEZ MAHMUD (Member, IEEE) received the B.Sc. degree in electrical and electronic engineering and the M.Eng. degree in mechatronics engineering. After the successful completion of his Ph.D. degree in engineering with several awards, including the Macquarie University Highly Commended Excellence in Higher Degree Research Award 2019, he worked as a Postdoctoral Research Associate and Academic with the School of Engineering, Macquarie University, Sydney. Besides, before coming to Australia, he worked as a Lecturer of mechatronics engineering with the World University of Bangladesh for more than two years and performed as a Researcher at the Korea Institute of Machinery and Materials for about three years. He is currently the Alfred Deakin Postdoctoral Fellow of the School of Engineering, Deakin University, Melbourne, VIC, Australia. He has made significant research contributions in the area of energy sustainability, energy harvesting, artificial intelligence, and smart sensing, and published more than 130 scholarly articles, including two authored books, nine book chapters, 86 peer-reviewed journal articles, and 39 fully refereed conference proceedings (Google Scholar). His one more full book proposal has already been accepted by Elsevier to be published in 2021. He is also supervising eight Ph.D. students in renewable energy, electric vehicles, advanced soft energy materials, energy sustainability, microgrid energy trading, machine learning, and artificial intelligence (AI). His research interests include energy materials, energy harvesting, smart sensing, and energy sustainability.

MD. FATIN ISHRAQUE received the B.Sc. degree in electrical and electronic engineering (EEE) from the Rajshahi University of Engineering and Technology, in 2018, where he is currently pursuing the M.Sc. degree. He is also working as a Lecturer with the Department of Electrical, Electronic and Communication Engineering (EECE), Pabna University of Science and Technology, Pabna, Bangladesh. His research interests include renewable energy, dispatch strategy, and IoT-based system designing.

SAJAL K. DAS received the Doctor of Philosophy (Ph.D.) degree in electrical engineering from the University of New South Wales, Australia, in 2014. He was appointed as a Research Engineer with the National University of Singapore (NUS), Singapore, in May 2014. He joined the Department of Electrical and Electronic Engineering, AIUB, as an Assistant Professor, in January 2015. He joined the Department of Mechatronics Engineering, Rajshahi University of Engineering and Technology (RUET), as a Lecturer, in September 2015. He is currently working as an Assistant Professor with RUET. His research interests include control theory and applications, mechatronics system control, robotics, and power system control.

MD RABIUL ISLAM SARKER received the bachelor's degree, and the M.Sc. degree in engineering from RUET and the Ph.D. degree from the University of Adelaide, Australia. He joined the positions of a Lecturer, an Assistant Professor, an Associate Professor, and a Professor, respectively. Since 2006, he has been actively engaged in a teaching position with the Faculty of Mechanical Engineering. He is currently teaching the core courses of mechanical engineering, including renewable energy engineering, fluid mechanics, fluid machinery, thermodynamics, engineering mechanics, mechanics of solids, refrigeration and air conditioning, solar energy engineering, and mechanical equipment's in both bachelor's and master's levels.

SK. A. SHEZAN received the Bachelor of Engineering degree in electrical engineering and automation from the Shenyang University of Chemical Technology, China, in 2013, the Master of Engineering degree from the University of Malaya, in 2016, and the Ph.D. degree in electrical and electronic engineering from RMIT University, Melbourne, VIC, Australia, in 2021. He was a Lecturer with the Electrical and Electronics Engineering Department, Uttara University, Dhaka, Bangladesh. He is currently working as a Lecturer with the Department of Electrical Engineering, Engineering Institute of Technology, Melbourne, Australia. His research interests include microgrid, HRES, solar energy, wind energy, optimization, power system analysis, and energy economics.

ZIAUR RAHMAN (Graduate Student Member, IEEE) received the bachelor's degree in software engineering at SUCT, China, and the master's degree in computer science from IUT, OIC. He is currently pursuing the Ph.D. degree in cybersecurity with RMIT University (City Campus), Melbourne, VIC, Australia, with full scholarship. He has been working as an Associate Professor (currently on study leave) at the Department of ICT, MBSTU, Bangladesh. He has been working as a Casual Research Assistant with Deakin University. Previously, he worked with RMIT, as a Casual Lecturer, as a CS Officer of RMIT Pro VC Office and worked with Monash University as a Casual Tutor in network security. His works received nomination and best paper award in the IEEE conferences and Elsevier journal. He is affiliated with ACM, ACS, and IEEE. His research interests include cybersecurity, machine learning, and software engineering.